articles

molecular pharmaceutics

Comparison of Reversible and Nonreversible Aqueous-Soluble Lipidized Conjugates of Salmon Calcitonin

Weiqiang Cheng[†,‡] and Lee-Yong Lim*[,§]

Department of Pharmacy, National University of Singapore, 18 Science Drive 4, Singapore 117543, and Pharmacy, School of Biomedical, Biomolecular and Chemical Sciences, University of Western Australia, 35 Stirling Highway, Crawley, WA 6009, Australia

Received January 30, 2008; Revised Manuscript Received April 13, 2008; Accepted April 16, 2008

Abstract: Reversible aqueous lipidization (REAL) at the interdisulfide bond has been shown to improve the deliverability of some peptide drugs. Recently, we developed a nonreversible aqueous lipidization method targeted at the interdisulfide bond of salmon calcitonin (sCT). The resultant derivative had comparable hypocalcemic activity to sCT after subcutaneous injection in rats, despite possessing significantly different biophysical properties. The purpose of this study was to conduct a comparative evaluation of the biophysical properties of the reversible aqueous-soluble lipidized sCT (REAL-sCT) and its corresponding nonreversible aqueous-soluble compound (Mal-sCT) with a view to correlate these properties to the bioactivities of the peptides. REAL-sCT and Mal-sCT were successfully synthesized, purified and identified. Both conjugates showed comparable retention times in a C-18 HPLC column, as well as robust helical structures and aggregation behavior in water, although REAL-sCT was shown by dynamic light scattering experiments to form larger aggregates than Mal-sCT in water. The larger particle size of REAL-sCT correlated with its stronger resistance to degradation by intestinal enzymes. Unlike Mal-sCT, REAL-sCT was rapidly converted to sCT in liver juice; however, the regenerated sCT appeared to degrade at a slower rate than unmodifed sCT in the liver juice. Compared with sCT, REAL-sCT after subcutaneous injection as an aqueous solution at a dose of 0.15 mg/kg produced a prolonged hypocalcemic activity that lasted at least 24 h in the rat. Using a novel LC-MS/MS method that was developed for this study, we were able to show concomitant increases in REAL-sCT and sCT plasma concentrations with time, the latter prevailing at 10% the molar concentration of the former. In contrast, sCT was not present in the plasma following the subcutaneous injection of Mal-sCT, although a comparable hypocalcemic activity with shorter duration was observed. Oral administration of REAL-sCT and Mal-sCT as aqueous solutions at sCT equivalent dose of 5.0 mg/kg did not produce significant hypocalcemic activity. This study is the first thorough examination of the biophysical characteristics of the corresponding reversible and nonreversible aqueous-soluble lipidized peptide molecules. The results obtained should be useful for the development of the oral formulation of peptide and protein drugs.

Keywords: Salmon calcitonin; lipidization; activity; characterization; delivery; pharmacokinetic; conjugation; disulfide

Introduction

Lipid conjugation is a promising method for increasing the deliverability of a peptide drug. The lipid can facilitate interaction between the peptide and its binding sites on the cell membrane, and promote a depot effect through binding to plasma proteins and the local administration site.[1,2] Lipid modification can also increase the enzymatic stability of the peptide drug.[3,4] Collectively, these properties may contribute

* Corresponding author. Mailing address: University of Western Australia, Pharmacy, School of Biomedical, Biomolecular and Chemical Sciences, 35 Stirling Highway, Crawley, WA 6009, Australia. E-mail: limly@cyllene.uwa.edu.au. Tel: 61-8-64884413. Fax: 61-8-64887532.

† National University of Singapore.

‡ Present address: Department of Pharmaceutical Sciences, University of Tennessee Health Science Center, 26 S Dunlap Street, Memphis, TN 38163.

§ University of Western Australia.

(1) Ellmerer, M.; Hamilton-Wessler, M.; Kim, S. P.; Dea, M. K.; Kirkman, E.; Perianayagam, A.; Markussen, J.; Bergman, R. N. Mechanism of action in dogs of slow-acting insulin analog O346. *J. Clin. Endocrinol. Metab.* **2003**, *88* (5), 2256–62.

(2) Havelund, S.; Plum, A.; Ribel, U.; Jonassen, I.; Volund, A.; Markussen, J.; Kurtzhals, P. The mechanism of protraction of insulin detemir, a long-acting, acylated analog of human insulin. *Pharm. Res.* **2004**, *21* (8), 1498–504.

10.1021/mp8000167 CCC: $40.75
Published on Web 05/16/2008

toward delayed systemic absorption and increased plasma circulation time, which can lead to prolonged or even enhanced efficacy. This is seen with insulin detemir [NN-304, also known as Lys B29-tetradecanoyl des-(B30) human insulin], a soluble, long-acting insulin which shows a flat time−action profile over 12 h and a long clearance rate from its subcutaneous injection site.[5] Likewise, stearoyl acylated antiviral antibodies have been observed to suppress virus reproduction by 100-fold greater than nonmodified antibodies because of their capacity for intracellular penetration.[6]

Despite its potential, lipidization frequently results in reduced or, in some cases, loss of bioactivity of a pharmaceutical.[7,8] To confer the benefits of lipidization without sacrificing efficacy, Shen's group designed a novel method, known as reversible aqueous lipidization (REAL), in which water-soluble lipid groups were conjugated to a peptide drug via interdisulfide bonds.[9−12] This method has been shown to be particularly useful for potentiating the activity of peptide drugs with an intradisulfide bond, such as desmopressin,[10,11] octreotide[13] and calcitonin.[12] The potentiated activities appeared to be related to the enhanced stability of the conjugates and their capacity to bind to local tissues and plasma proteins and the regeneration of the parent drug in vivo. However, despite many successful examples, there has been little detailed research on the biophysical properties of REAL-lipidization on a peptide drug.

Recently, we developed a nonreversible aqueous-based lipid modification method targeted at the intradisulfide bond of a peptide drug.[14] The argument for nonreversible lipidization is that it maintains greater conjugate stability, and therefore greater assurance of realizing the lipid-mediated advantages in vivo compared to a labile lipid conjugate. Further literature research also showed that the intradisulfide bond is frequently not essential for activity of peptide drugs containing such bonds, examples of which included desmopressin,[15] octreotide,[16,17] and salmon calcitonin.[18] When we modified salmon calcitonin by this nonreversible lipidization method, the resulting product, Mal-sCT, showed similar in vivo hypocalcemic activity as unmodified sCT after subcutaneous injection in the rat.[14] The level of bioactivity was comparable on a dose basis with the reported bioactivity of REAL-sCT;[12] however, unlike REAL-sCT, which required formulation into an emulsion, the bioactivity of Mal-sCT was realized using water as the vehicle. The comparable bioactivity between REAL-sCT and Mal-sCT was intriguing because, despite the many reports on reversible lipidization of peptide drugs, there has been no comparative evaluation of reversible versus nonreversible lipidization at the interdisulfide bonds of a peptide drug on its properties and deliverability. We have shown Mal-sCT to exhibit unique biophysical properties with regard to aggregation status, secondary structure, cellular uptake and stability against liver enzyme degradation relative to unmodified sCT. It would be interesting to determine if REAL lipidization would result also in similar changes in these biophysical properties.

In this paper, salmon calcitonin (Figure 1A) as the model peptide drug was transformed into the reversible lipidized peptide, REAL-sCT (Figure 1B), and the corresponding

(3) Wang, J.; Shen, W. C. Gastric retention and stability of lipidized Bowman-Birk protease inhibitor in mice. *Int. J. Pharm.* **2000**, *204* (1−2), 111–6.
(4) Delie, F.; Couvreur, P.; Nisato, D.; Michel, J. B.; Puisieux, F.; Letourneux, Y. Synthesis and in vitro study of a diglyceride prodrug of a peptide. *Pharm. Res.* **1994**, *11* (8), 1082–7.
(5) Markussen, J.; Havelund, S.; Kurtzhals, P.; Andersen, A. S.; Halstrom, J.; Hasselager, E.; Larsen, U. D.; Ribel, U.; Schaffer, L.; Vad, K.; Jonassen, I. Soluble, fatty acid acylated insulins bind to albumin and show protracted action in pigs. *Diabetologia* **1996**, *39* (3), 281–8.
(6) Kabanov, A. V.; Ovcharenko, A. V.; Melik-Hubarov, N. S.; Bannikov, A. I.; Alakhov, V.; Kiselev, V. I.; Sveshnikov, P. G.; Kiselev, O. I.; Levashov, A. V.; Severin, E. S. Fatty acid acylated antibodies against virus suppress its reproduction in cells. *FEBS Lett.* **1989**, *250* (2), 238–40.
(7) Asada, H.; Douen, T.; Mizokoshi, Y.; Fujita, T.; Murakami, M.; Yamamoto, A.; Muranishi, S. Stability of acyl derivatives of insulin in the small intestine: relative importance of insulin association characteristics in aqueous solution. *Pharm. Res.* **1994**, *11* (8), 1115–20.
(8) Hashimoto, M.; Takada, K.; Kiso, Y.; Muranishi, S. Synthesis of palmitoyl derivatives of insulin and their biological activities. *Pharm. Res.* **1989**, *6* (2), 171–6.
(9) Ekrami, H. M.; Kennedy, A. R.; Shen, W. C. Water-soluble fatty acid derivatives as acylating agents for reversible lipidization of polypeptides. *FEBS Lett.* **1995**, *371* (3), 283–6.
(10) Wang, J.; Shen, D.; Shen, W. C. Preparation, purification, and characterization of a reversibly lipidized desmopressin with potentiated anti-diuretic activity. *Pharm. Res.* **1999**, *16* (11), 1674–9.
(11) Wang, J.; Wu, D.; Shen, W. C. Structure-activity relationship of reversibly lipidized peptides: studies of fatty acid-desmopressin conjugates. *Pharm. Res.* **2002**, *19* (5), 609–14.
(12) Wang, J.; Chow, D.; Heiati, H.; Shen, W. C. Reversible lipidization for the oral delivery of salmon calcitonin. *J. Controlled Release* **2003**, *88* (3), 369–80.
(13) Yuan, L.; Wang, J.; Shen, W. C. Reversible lipidization prolongs the pharmacological effect, plasma duration, and liver retention of octreotide. *Pharm. Res.* **2005**, *22* (2), 220–7.
(14) Cheng, W.; Satyanarayanajois, S.; Lim, L. Y. Aqueous-soluble, non-reversible lipid conjugate of salmon calcitonin: synthesis, characterization and in vivo activity. *Pharm. Res.* **2007**, *24* (1), 99–110.
(15) Cort, J. H.; Schuck, O.; Stribrna, J.; Skopkova, J.; Jost, K.; Mulder, J. L. Role of the disulfide bridge and the C-terminal tripeptide in the antidiuretic action of vasopressin in man and the rat. *Kidney Int.* **1975**, *8* (5), 292–302.
(16) Gazal, S.; Gelerman, G.; Ziv, O.; Karpov, O.; Litman, P.; Bracha, M.; Afargan, M.; Gilon, C. Human somatostatin receptor specificity of backbone-cyclic analogues containing novel sulfur building units. *J. Med. Chem.* **2002**, *45* (8), 1665–71.
(17) Afargan, M.; Janson, E. T.; Gelerman, G.; Rosenfeld, R.; Ziv, O.; Karpov, O.; Wolf, A.; Bracha, M.; Shohat, D.; Liapakis, G.; Gilon, C.; Hoffman, A.; Stephensky, D.; Oberg, K. Novel long-acting somatostatin analog with endocrine selectivity: potent suppression of growth hormone but not of insulin. *Endocrinology* **2001**, *142* (1), 477–86.
(18) Orlowski, R. C.; Epand, R. M.; Stafford, A. R. Biologically potent analogues of salmon calcitonin which do not contain an N-terminal disulfide-bridged ring structure. *Eur. J. Biochem.* **1987**, *162* (2), 399–402.

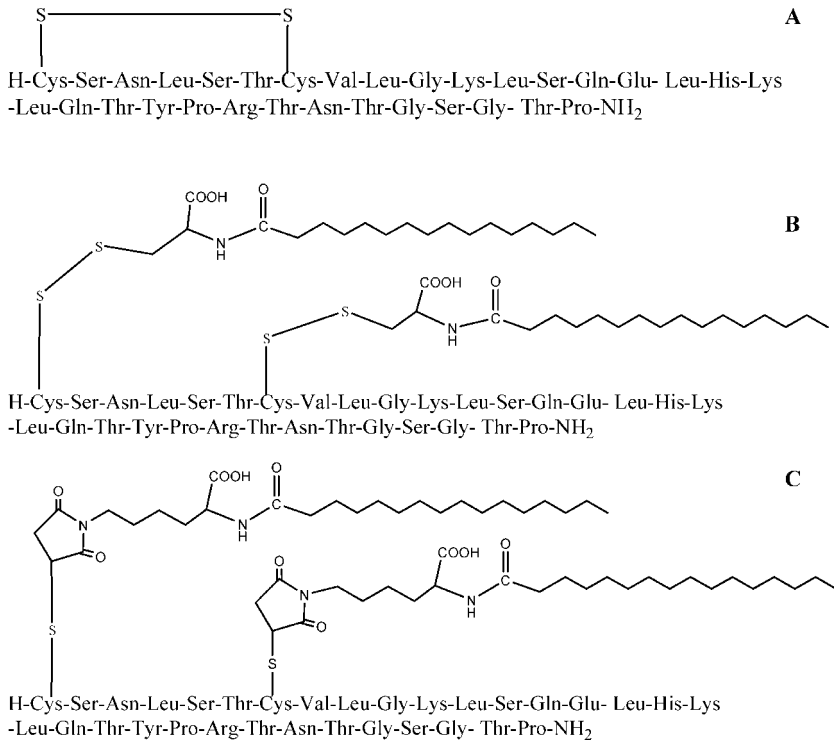

Figure 1. Chemical structure of (A) salmon calcitonin, (B) reversible aqueous lipidized salmon calcitonin (REAL-sCT) and (C) nonreversible aqueous lipidized sCT (Mal-sCT).

nonreversible lipidized peptide, Mal-sCT (Figure 1C), using the palmitoyl lipid chain. The aqueous-soluble sCT-lipid conjugates were comparatively evaluated for lipophilicity, aggregation in aqueous media, structural conformation, pharmacokinetic profiles and bioactivity after subcutaneous and oral administration. To our knowledge, this is the first comparative study on a REAL lipidized peptide with its nonreversible counterpart in vitro and in vivo. The data obtained should help to address the issue of whether reversible or irreversible lipidation offers greater potential toward improving the deliverability of peptide drugs.

Materials and Methods

sCT was from Unigene Laboratory (New Jersey); cysteine hydrochloride, 3,3′-dithiobis-pyridine dithiodipyridine (DTDP), palmitic acid, trifluoroacetic acid (TFA), palmitic acid *N*-succinimidyl ester (Pal-Suc), trifluoroethanol, methylpyrrolecarboxylate, tris(2-carboxyethyl) phosphine (TCEP), and calcium standard solution (1.000 mg/mL) were from Sigma-Aldrich (St. Louis, MO); and the MicroBCA Protein Assay Kit was from Pierce Biotechnology (Rockford, IL). Acetonitrile and isopropanol of high pressure liquid chromatography (HPLC) grade, cyclohexane, chloroform and acetone of analytical grade were supplied by Fisher Scientific (Irvine, CA). Milli-Q water was used in the mobile phase for HPLC analysis.

Finnegan MAT LCQ mass spectrometer, equipped with an Electrospray Ionization (ESI) or Atmospheric Pressure Chemical Ionization (APCI) source, and coupled with Xcalibur LCQ Tune Plus Version 1.0 SR software (San Jose, CA), was used for qualitative mass spectrometry analysis. The MS spectrometer settings were as follows: capillary temperature 270 °C; sheath gas 75 unit/min; auxiliary gas 20 unit/min, spray voltage 4 kV, capillary voltage 10 V. LC flow rate: 0.5 mL/min (50% methanol). Injection volume: 20 μL. Plasma samples in the pharmacokinetic study were analyzed using the Q-TRAP LC−MS/MS system (Applied Biosystems Inc. CA).

Chemical Syntheses. REAL-sCT. REAL-sCT was synthesized according to published methods,[9,19] with slight modifications. Briefly, DTDP was reacted with cysteine to generate the target product, cysteinyl pyridyl disulfide (CPD). CPD and Suc-Pal were further reacted to yield the palmitoyl derivative of cysteinyl pyridyl disulfide (Pal-CPD). REAL-sCT was synthesized when Pal-CPD solution was reacted with reduced sCT, prepared by reacting sCT with DTT. REAL-sCT was purified in a semipreparative C-18 HPLC column and the purified compound was identified using electrospray ionization mass spectrometry (ESI-MS). The theoretical MW of REAL-sCT (4149.0 Da) was calculated using ChemDraw Ultra 8.0 (CambridgeSoft Corporation, MA).

Mal-sCT. Mal-sCT was synthesized as described previously.[14] Briefly, a water-soluble ϵ-maleimido lysine derivative of palmitic acid was synthesized by reacting Pal-Suc with ϵ-maleimido lysine. The latter was generated from a reaction of α-Boc-lysine and methylpyrrolecarboxylate, with subsequent deprotection of the Boc group by anhydrous

(19) Carlsson, J.; Drevin, H.; Axen, R. Protein thiolation and reversible protein-protein conjugation. N-Succinimidyl 3-(2-pyridyldithio) propionate, a new heterobifunctional reagent. *Biochem. J.* **1978**, *173* (3), 723–37.

hydrochloride. The palmitic derivative was further conjugated with sCT via a thio-ether bond to produce Mal-sCT in aqueous solution under reductive condition maintained by TCEP. Mal-sCT was purified using the HPLC and identified using ESI-MS.

Fractions containing purified REAL-sCT and Mal-sCT were pooled together, and the solvent was evaporated off at room temperature in a rotary evaporator to yield a final conjugate concentration of 1.0−2.0 mg/mL, The concentrated eluents were frozen at −80 °C and freeze-dried (FD8 Dynavac freeze drier). The purity of REAL-sCT and Mal-sCT was confirmed by HPLC analysis (Hewlett-Packard 1050 HPLC system equipped with Hewlett-Packard 1100 autosampler) and carried out using a Waters Symmetry 300 C-18 column (4.6 × 250 mm). Elution time profile was from 100% A: water (0.1% TFA) to 100% B: 1:1 v/v mixture of isopropanol and acetonitrile (0.1% TFA) in 40 min, maintaining at 100% B for another 5 min. Volume of sample injected was 100 μL and the sample was detected at λ = 214 nm. Baseline was corrected by subtracting the chromatography of samples with that of a blank injection.

Peptide Conformation. Peptide conformation was determined by circular dichroism (CD). CD spectra were obtained with a Jasco circular dichroism system 810 over a scanning range of 190 to 260 nm. The N_2 flow rate was set at 5 L/min. The sample cuvette (200 μL) was cleaned until blank samples (0, 20 and 50% of trifluoroethanol (TFE) in water) showed optical density of less than 0.5 mdeg. The spectra of test samples, which comprised 0.10 mM of sCT or sCT conjugate dissolved in distilled water containing 0−50% of TFE, were recorded with the corresponding solvents serving as blanks.

Morphology. The morphology of sCT, Mal-sCT, 1PEG-Mal-sCT and 2PEG-Mal-sCT was visualized by transmission electron microscopy (TEM, JEOL JEM-2010, Japan). Samples were dissolved in water to a concentration of 0.5 mM, and 2 μL of each solution was mixed with 1 μL of 1% phosphotungstic acid solution for about 1 min on a TEM grid. Excess solution was blotted with fiber-free tissue paper, and the samples were dried under ambient conditions before they were observed under the TEM.

Particle Size. Particle size was determined using the Protein Solutions DynaPro dynamic light scattering instrument (Wyatt Technology Corporation, Santa Barbara, CA) at a laser wavelength of 825.8 nm, detector angle of 90°, and typical sample volume of 20 μL. Each light scattering experiment consisted of 20 or more independent measurements, and the data were analyzed using the DynaPro software, DYNAMICS (version 5.26.60). Samples were dissolved in distilled water at concentrations of 2.5, 11, 50, 220 and 1000 μM. To minimize dust interference, all solutions were freshly prepared and centrifuged at 2000 rpm for 2 min (Eppendorf centrifuge 5417, Hamburg, Germany) immediately prior to analysis.

Stability to Enzymatic Degradation. Stability of the peptides in intestinal fluid was determined according to a published method,[20] with slight modification. To obtain the intestinal fluid, 3 female Wistar rats (9 weeks, about 220 g), which had been fasted for 24 h, were euthanized by intraperitoneal (IP) injection of ketamine (150 mg/kg) and xylazine (20 mg/kg). The intestine was exposed by an abdominal incision, and 30−40 cm of the small intestine, beginning from the duodenum, was excised and the luminal content flushed out with 7.5−9.0 mL of phosphate buffer solution (PBS, pH 6.6) using a syringe (actual intestinal fluid volume was approximately 0.5−1.5 mL). The protein content in the intestinal fluid was determined by the MicroBCA protein assay kit (Pierce Biotechnology, Rockford, IL). Protein contents in the intestinal fluids of the 3 rats were found to be 1.32, 1.27 and 1.47 mg/mL, respectively. The intestinal fluids were further diluted with 0.1 M of pH 6.6 PBS to yield a final protein content of 0.9 mg/mL. The degradation experiments were initiated by adding 30 μL of intestinal fluid (0.9 mg/mL) to 566 μL of peptide (43 μM) in pH 6.6 PBS at 37 °C to yield final intestinal protein content of 45 μg/mL. At specific time points, aliquots of the digested mix were withdrawn and the enzyme activity was quenched by lowering the pH to 2.5 through the addition of glacial acetic acid. The mixture was then analyzed using the HPLC.

To determine the stability of the peptides against hepatic metabolism, a study was conducted using a previously described *in vitro* metabolic system[11] with slight modification. A fresh liver (7.5 g), harvested from a euthanized normal Wistar female rat (240 g), was soaked in normal saline, then triturated and mixed with 7.5 mL of ice-cold MEM solution containing 5% FBS. The mixture was centrifuged at 2000 rpm at 4 °C (Hettich Zentrifugen, Tuttlingen, Germany) for about 2 min, and the supernatant was collected. Lyophilized sCT and sCT conjugates were separately added to aliquots of the supernatant to give final concentrations of 0.10 mM, and the mixtures were incubated in a water bath operating at 37 °C and a shaking frequency of 60 rpm. The reacting mixtures were sampled at 0, 15, 30, 45, 60, 90, and 120 min. Ethanol (125 μL) was immediately added, under vortex, to each withdrawn sample (50 μL) to quench the reaction, and the supernatant fractions (120 μL), isolated by centrifugation of the samples, were analyzed by HPLC.

In Vivo Hypocalcemic Activity. Pharmacodynamic response of sCT and the sCT conjugates was evaluated by analysis of plasma calcium concentration in the rat model.[21] Wistar female rats weighing 170−220 g (about 8 weeks old) were purchased from the National University of Singapore (NUS) Centre for Animal Resources, and housed at the NUS

(20) Mansoor, S.; Youn, Y. S.; Lee, K. C. Oral delivery of mono-PEGylated sCT (Lys18) in rats: regional difference in stability and hypocalcemic effect. *Pharm. Dev. Technol.* **2005**, *10* (3), 389–96.

(21) Sinko, P. J.; Smith, C. L.; McWhorter, L. T.; Stern, W.; Wagner, E.; Gilligan, J. P. Utility of pharmacodynamic measures for assessing the oral bioavailability of peptides. 1. Administration of recombinant salmon calcitonin in rats. *J. Pharm. Sci.* **1995**, *84* (11), 1374–8.

Animal Holding Unit. All experimental protocols involving animals were approved by the NUS Animals Ethics Committee. The rats were divided randomly into groups of 6 after 3 days of acclimatization, and the pharmacodynamic response was assessed following subcutaneous and oral administration of the peptides.

For subcutaneous administration, sCT, REAL-sCT and Mal-sCT were separately dissolved in water and injected under the dorsal skin of the rat using a 27-gauge needle at a dose of 0.15 mg/kg. For oral administration, the peptides were separately dissolved in distilled water to give 2.5 mg/mL sCT equivalent solutions. The rats were fasted for 12−16 h before they were administered by intragastric gavage via an 18-gauge gavage needle with 5.0 mg/kg of sCT, 6.1 mg/kg of REAL-sCT or 6.4 mg/kg of Mal-sCT (equivalent to 5.0 mg/kg of sCT). Control rats were administered with an equivalent volume of water (200 μL). Immediately before, and at 1, 2, 4, 8, 12, 18, 24, 36, 48 h after administration, blood samples (120−150 μL) were collected via either tail vein or saphenous vein puncture with a Microvette CB300LH (Sarstedt, Germany). Blood plasma was obtained by centrifuging the samples at 5000 rpm (Eppendorf centrifuge 5145D) for 5 min at 15 °C.

Plasma calcium level was assayed by atomic absorption spectrometry (Perkin-Elmer AAnalyst 100, MA) using a hollow calcium lamp at $\lambda = 422.7$ Å as the light source.[22] Slit width was 0.7 nm and pure ethyne/compressed air flame was used. Calibration was performed using standard solutions that contained 5.0, 10.0 and 15.0 mg/dL of calcium, together with 140 mM of NaCl and 5 mM of KCl. Blank solutions comprised 140 mM of NaCl and 5 mM of KCl without calcium. The standard and blank solutions, as well as all plasma samples, were diluted 50-fold with a solution containing 10 mM of $LaCl_3$ and 37 mM of HCl before they were analyzed. Average recovery of calcium using this method was 100.3% (RSD = 3.8%, $n = 3$) over the concentration range of 5.55 to 13.3 mg/dL.

Pharmacokinetics Profile. Wistar female rats weighing 180 to 220 g were randomly assigned to 3 treatment groups, and injected subcutaneously (27-gauge needle) with 0.44 μmol/kg of sCT (1.50 mg/kg, 1.50 mg/mL), REAL-sCT (1.81 mg/kg, 1.81 mg/mL) or Mal-sCT (1.90 mg/kg, 1.90 mg/mL) in normal saline. At predetermined time, 50 μL of blood was withdrawn from each rat by saphenous vein puncture and collected with a Microvette CB300LH (Sarstedt, Germany). The blood samples were immediately centrifuged at 5000 rpm for 5 min to obtain 20 μL of plasma. Plasma samples were stored at −80 °C until analysis. Samples to be analyzed by LC−MS/MS were thawed at ambient temperature, diluted with an equal volume (20 μL) of water and then mixed with 80 μL of ACN−IPA under vortex to precipitate the plasma protein. The precipitate was pelleted by centrifugation at 5000 rpm, and the clear supernatant (30 μL) was immediately injected into the LC−MS for peptide analysis.

LC−MS/MS settings consisted of a Q-TRAP MS instrument (Applied Biosystems) coupled with an Agilent 1100 HPLC system (Agilent Technologies). A Waters Symmetry 300 C-4 (2.1 × 150 mm, particle size 5 μm, 300 Å) column was used for detecting sCT, REAL-sCT and Mal-sCT. The LC gradient was from 10% to 90% ACN−IPA (1:1 v/v) mixture in water (containing 0.1% formic acid) in 12 min and further to 100% ACN−IPA mixture in another 3 min, then gradually returned to 10% of ACN−IPA by 27 min. The column oven was set at 35 °C, and the eluent before 8 min and after 16 min was diverted to waste container. The multiple reaction monitoring (MRM) signals were optimized to give the strongest response; the final settings for sCT were optimized to detect parent ion 858.6 ($M + 4H^+$) and its daughter ion 115.1; for REAL-sCT, the final settings detected the parent ion 1038.0 ($M + 4H^+$) and its daughter ion 115.1, while for Mal-sCT, the final settings detected the parent ion 1091.5 ($M + 4H^+$) and its daughter ion 115.1. During analysis of REAL-sCT and Mal-sCT, the ion pair for detecting sCT was also input to simultaneously determine any sCT released from the conjugates. Plasma solutions containing known concentrations (2.5 nM to 500 nM) of sCT, REAL-sCT and Mal-sCT showed good linearity and reproducibility.

Results

Synthesis and Identification. The identities of REAL-sCT and Mal-sCT were confirmed by ESI-MS mass spectrometry (not shown). In the case of REAL-sCT (calculated MW 4149.0 Da), the observed m/z peaks of 830.6 (9%), 1038.3 (100%) and 1384.1 (15%) corresponded closely to the m/z values of 830.8 ($M + 5H^+$), 1038.3 ($M + 4H^+$), and 1384.0 ($M + 3H^+$), calculated using the formula $m/z = (M + nH^+)/n$. Similarly, the observed peaks of 873.5 (15%), 1091.4 (100%) and 1454.5 (5%) matched well with the m/z values of 873.5 ($M + 5H^+$), 1091.1 ($M + 4H^+$), and 1454.5 ($M + 3H^+$) calculated on the basis of a theoretical MW of 4360.4 Da for Mal-sCT.

To confirm that the lipid molecules in REAL-sCT were conjugated via disulfide bonds, REAL-sCT and sCT (0.05 μM) were separately incubated under reductive conditions maintained by DTT at ambient temperature. REAL-sCT after reduction did not show peaks at 830.8, 1038.3 and 1384.0. Instead, new peaks (result not shown) were observed at m/z values of 687.6, 859.2, 1145.0 and 1718.4, which corresponded with the calculated m/z values for $M + 4H^+$, $M + 3H^+$ and $M + 2H^+$of reduced sCT (MW 3433.9). The data confirmed that REAL-sCT was successfully synthesized through disulfide conjugation bonds.

Purity and Hydrophobicity. HPLC analyses of the REAL-sCT and Mal-sCT samples yielded single peaks (Figure 2), suggesting that they were highly purified. sCT had the shortest retention time (t_R) of 21.5 min, while both

(22) Van Loon, J. C. *Analytical atomic absorption spectroscopy: selected methods*; Academic Press: New York, 1980; p xi; 337 pp.

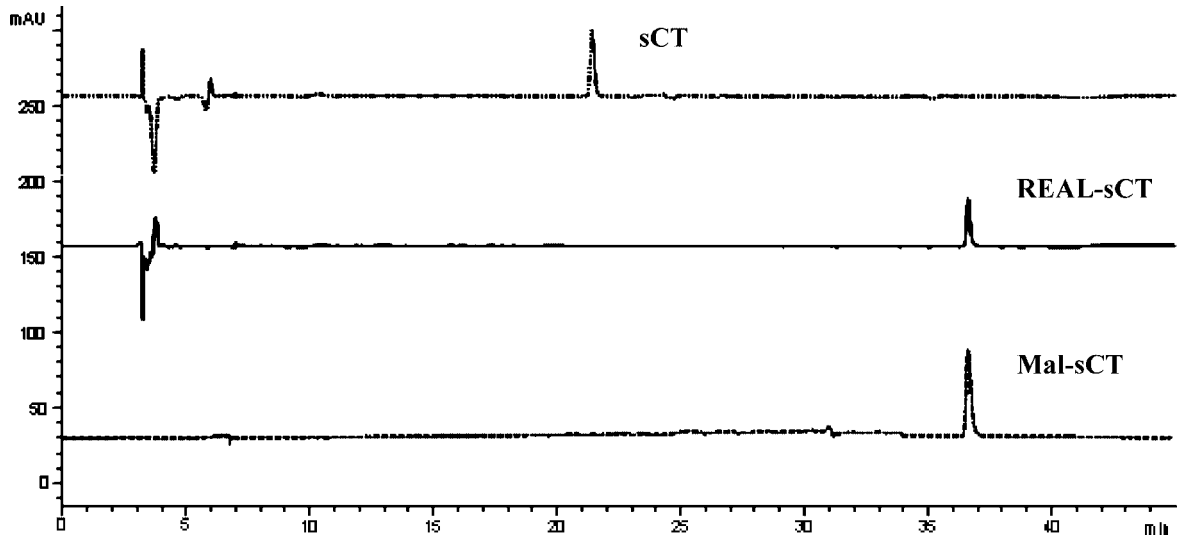

Figure 2. HPLC chromatographs of sCT, REAL-sCT and Mal-sCT.

REAL-sCT and Mal-sCT were eluted at 36.8 min, suggesting that the two lipidized sCT had comparable lipophilicities.

Peptide Conformation. The CD spectra of sCT in water showed no apparent secondary structure (Figure 3A). Upon the addition of TFE, an organic solvent with low dielectric constant, sCT showed a positive peak at 192 nm and 2 negative peaks at 208 and 222 nm, respectively, suggesting the presence of a helical structure. This structure became more evident at higher TFE concentrations. In contrast, REAL-sCT (Figure 3B) and Mal-sCT (Figure 1C) exhibited comparable CD spectra whether they were dissolved in water or in aqueous solutions of TFE, indicating that both sCT conjugates had stable helical conformations that were less dependent on the environment than the conformation of unmodified sCT.

Morphology. Figure 4 shows the TEM micrographs of sCT, REAL-sCT and Mal-sCT. At a magnification of 10,000×, sCT appeared as a relatively homogeneous dispersion (Figure 4A). REAL-sCT (Figure 4B) and Mal-sCT (Figure 4C) samples, on the other hand, were not homogeneous, showing instead evidence of widespread clumping, the two sCT conjugates exhibiting slightly different aggregation patterns. It should be borne in mind, however, that while the micrographs suggest agglomeration of REAL-sCT and Mal-sCT in water, the samples were viewed after vacuum drying, and artifacts could have been introduced during the sample processing.

Particle Size. To confirm the agglomeration propensity of the peptide conjugates, sCT and its lipidized derivatives in solution were subject to particle size analysis using dynamic light scattering. sCT (MW 3.43 kDa) at the concentrations of 224 and 1000 μM in distilled water showed dominant peaks (>99%) corresponding to mean radii of 0.99 and 1.1 nm (Figure 5). These translated to MW of 3.25 and 4.20 kDa (DYNAMICS Version 5.26.60), respectively, which was comparable with the calculated MW of sCT, suggesting that sCT in distilled water existed mainly as monomers. The implication was that sCT showed negligible

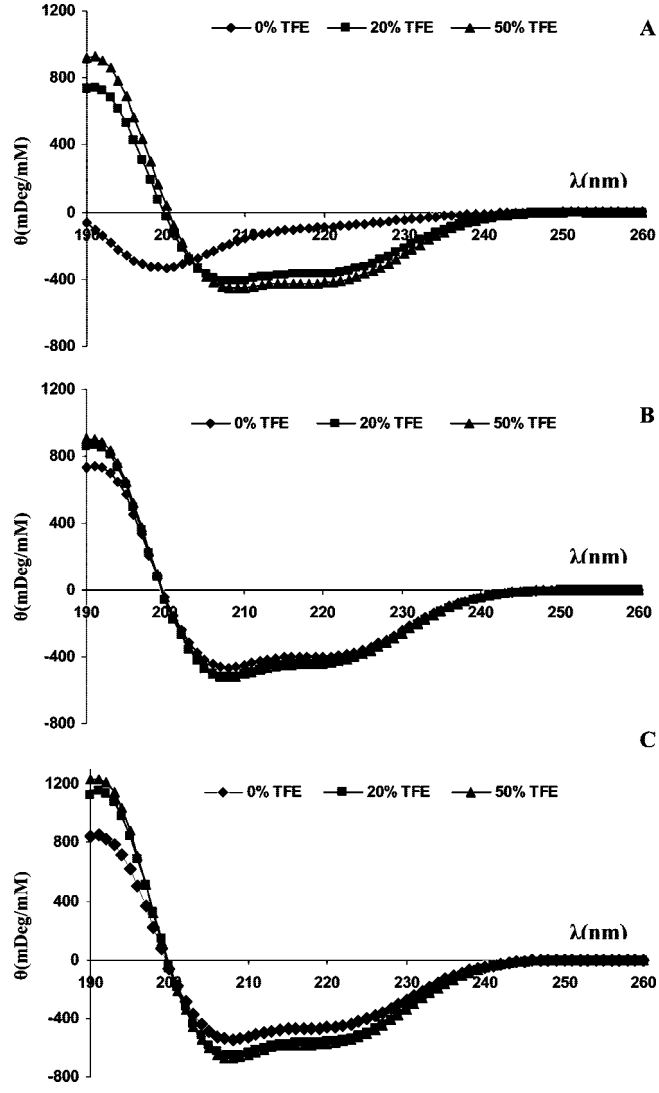

Figure 3. Circular dichroism spectra of (A) sCT, (B) REAL-sCT and (C) Mal-sCT in aqueous solutions containing different concentrations of trifluoroethanol (TFE).

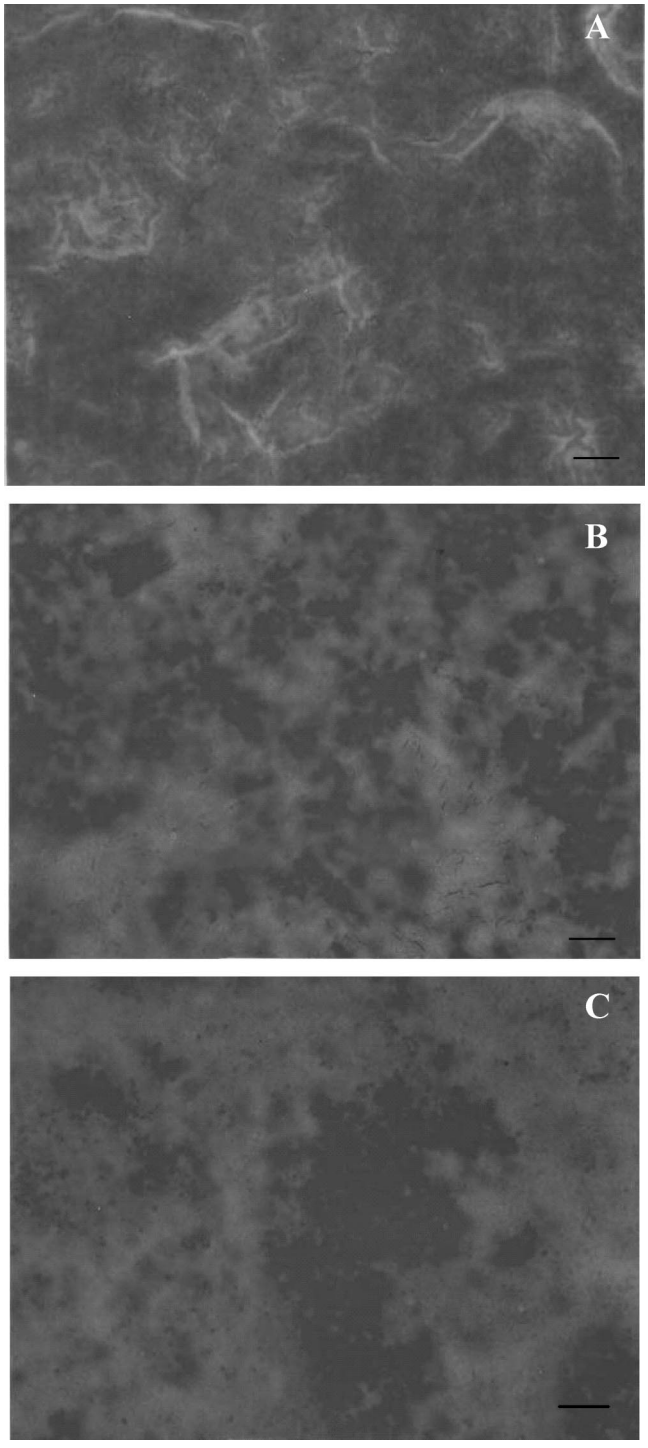

Figure 4. TEM micrographs of (A) sCT, (B) REAL-sCT and (C) Mal-sCT. Samples were prepared by mixing 2 μL of peptide solution (0.5 mM in water) with 1 μL of 1% phosphotungstic acid solution for 1 min in a TEM grid. Magnification 10,000×; scale bar, 500 nm.

tendency to aggregate when dissolved in water at these two concentrations. Further dilution of the sCT solution to 50 and 2.5 μM resulted in very low photon counts of less than 20 kcps, comparable to that of distilled water, which made it difficult to take measurements against the background noise.

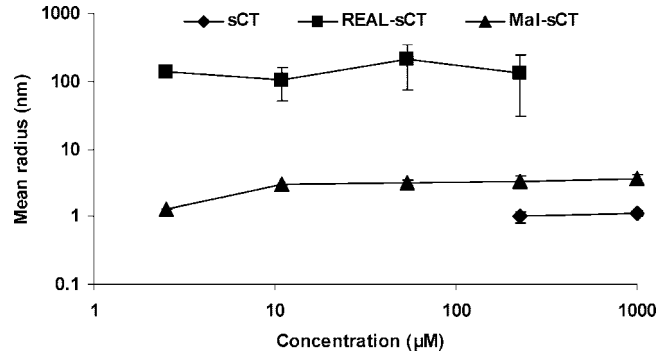

Figure 5. Dominant particle size (more than 98% mass) as a function of concentration of sCT, REAL-sCT and Mal-sCT in water, as measured by dynamic light scattering. Data represent mean ± polydispersity of at least 20 scans.

By comparison, Mal-sCT (MW 4.36 KDa) had a predominant peak (>99% by mass) at mean radii of 3.1 to 3.6 nm over a wide concentration range of 11.2 to 1000 μM. The particle size range was equivalent to a calculated MW of between 46.02 and 66.37 KDa. Further dilution of the Mal-sCT solution to 2.5 μM resulted in a hydrodynamic radius of 1.3 nm, equivalent to 6.38 KDa, or 1.5 times the MW of Mal-sCT. These data suggest that Mal-sCT in aqueous solutions might have transited from aggregated to monomeric states when diluted from 11.2 to 2.5 μM.

In contrast, REAL-sCT (MW 4.15 kDa) particles had a dominant peak at mean radii of 105 to 134.3 nm over the concentration range of 2.5 to 224 μM in water. The particle size of REAL-sCT could not be determined at the higher concentration of 1.0 mM as the photon count was beyond the upper limit of measurement (8000 kcps) of the equipment. As these radii were larger than the expected radius of 1.1−1.2 nm based on the calculated MW of the REAL-sCT monomer, aggregation of REAL-sCT into much larger particles than those observed for Mal-sCT was implicated. The wider polydispersity of REAL-sCT also indicated that the peptide did not form uniformly sized aggregates in solution.

Enzymatic Stability. The degradation data for sCT and Mal-sCT in the rodent liver juice fitted a first order profile to give the following respective equations: $Y = 100e^{-0.231t}$ ($R^2 = 0.91$) and $Y = 100e^{-0.0195t}$ ($R^2 = 0.92$), where Y represents the percent remaining after incubation. The control sCT sample was degraded rapidly, with less than 1% remaining in 15 min (Figure 6), while a comparison of the two equations suggests that Mal-sCT was 11.8-fold more resistant than sCT against liver metabolism. In the case of REAL-sCT, HPLC analysis of the digestion mix showed sCT to be generated immediately upon incubation with the liver homogenate whereas REAL-sCT was below detection limit. Significantly, the peak area corresponding to the regenerated sCT proceeded to decline at a slower rate than that for unmodified sCT, alluding to a continuous release of sCT from the REAL-sCT to replace the sCT that was metabolized by the liver enzymes. This was in spite of the lack of a definitive peak for REAL-sCT in the chromatogram. The sCT peak could be attributed to the reductive conditions provided

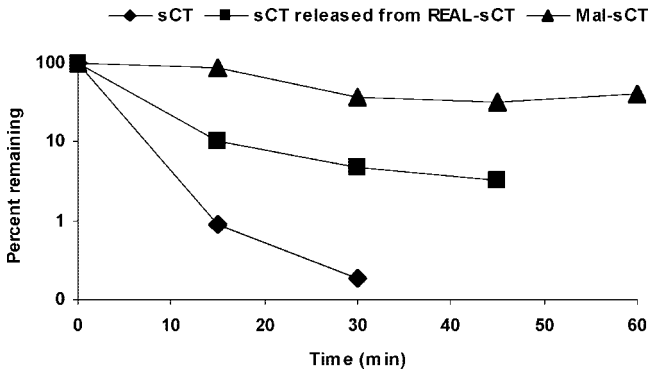

Figure 6. Percent remaining of sCT, sCT from REAL-sCT, Mal-sCT when incubated with fresh liver extract. Liver extract was the turbid supernatant obtained by centrifuging a mixture of homogenized rat liver (7.5 g) and 7.5 mL of MEM (with 5% FBS).

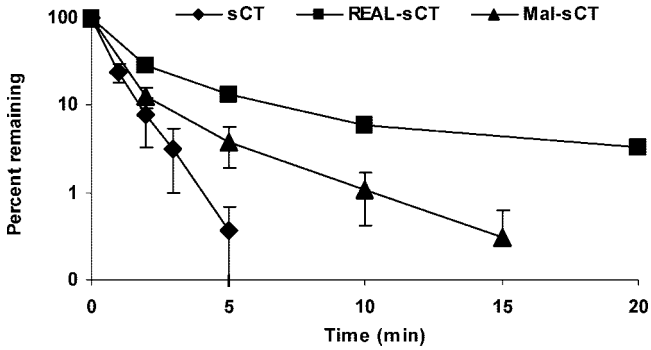

Figure 7. Degradation of sCT, REAL-sCT and Mal-sCT in rat intestinal solution. sCT and its conjugates (40 μM) were separately incubated with diluted rat intestinal fluid (45 μg protein/mL) at 37 °C at agitation rate of 50 rpm, $n = 3$.

by the liver homogenate, which cleaved the inter-disulfide bonds in REAL-sCT to release the reduced sCT with 2 thiol groups from the conjugated lipids. The reduced sCT later yielded original sCT with an intra-disulfide bond due to auto-oxidization of the two thiol groups in air. Thus, the peak intensity of REAL-sCT became too low to be detectable from background noise. Failure to detect REAL-sCT in the liver homogenate was unlikely to be caused by inefficient extraction because Mal-sCT, which had similar lipophilicity, was extracted in significant amounts. Moreover, REAL-sCT was readily detected in samples incubated with intestinal homogenates (Figure 7). The latter appeared incapable of reducing REAL-sCT to sCT, thus confirming its oxidative environment[23] relative to liver homogenates. In comparison, sCT was not generated from Mal-sCT following liver juice incubation, although the Mal-sCT peak showed a slower rate of decline compared to the sCT peak generated from REAL-sCT. The absence of sCT in the Mal-sCT−liver homogenate samples suggested that sCT was bound to the lipid in a nonreversible manner in Mal-sCT.

(23) Kurtel, H.; Granger, D. N.; Tso, P.; Grisham, M. B. Vulnerability of intestinal interstitial fluid to oxidant stress. *Am. J. Physiol.* **1992**, *263* (4 Part 1), G573–8.

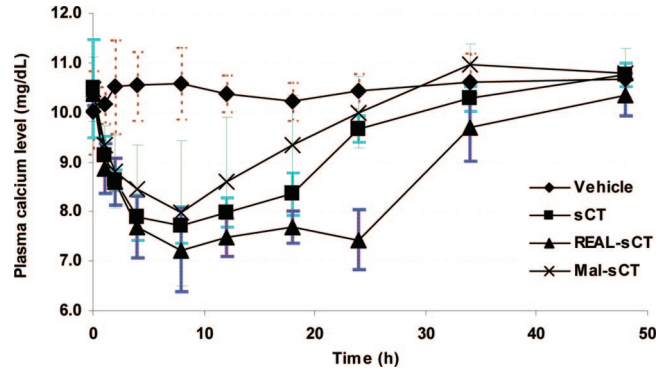

Figure 8. Plasma calcium level of Wistar female rats administered with sCT, REAL-sCT and Mal-sCT by subcutaneous injection. sCT and the conjugates were administered as 0.15 mg/mL in distilled water at the dose of 0.15 mg/kg. Data represent mean ± SD ($n = 6$).

Figure 7 shows the degradation profiles of sCT, REAL-sCT and Mal-sCT in the diluted rodent intestinal fluid. Incubation of sCT with the intestinal fluid resulted in less than 1% of the peptide remaining at 5 min, the degradation−time profile following first order kinetics ($Y = 100e^{-1.15x}$, $R^2 = 0.99$). In contrast, the corresponding degradation data of REAL-sCT and Mal-sCT did not fit into first order kinetics ($R^2 < 0.85$). The lipidized peptides showed rapid degradation in the initial 2 min, in which more than 60% of the peptides were digested, followed by slower rates of degradation over the next 18 min. At 2 and 5 min, the percentages remaining for Mal-sCT were not significantly different from those for sCT, but REAL-sCT was significantly more resilient.

In Vivo Hypocalcemic Activity. The hypocalcemic activities of subcutaneously administered Mal-sCT and REAL-sCT were evaluated in the rat model with sCT as control. Rats in all groups, including those administered with water, did not show significantly different baseline plasma calcium levels (10.0−10.5 mg/dL) (Figure 8). Neither did the plasma calcium level vary significantly from baseline level for 48 h after the subcutaneous administration of water. In contrast, there was a sustained, comparable lowering of plasma calcium level up to 18 h for rats in the sCT and Mal-sCT treatment groups, which was in agreement with published data.[24] Rats administered subcutaneously with equivalent concentration of REAL-sCT had comparable plasma calcium levels to those in the sCT treatment group in the initial 18 h ($p > 0.3$). However, REAL-sCT showed a longer duration of action, sustaining lower plasma calcium levels ($p < 0.01$) at 24 h after administration. Plasma calcium levels reverted to baseline levels by 36 h in all 3 treatment groups.

The biological activities of peroral sCT, REAL-sCT and Mal-sCT were also compared. All 6 rats administered with sCT (dose 5.0 mg/kg) by intragastric gavage showed significantly lower plasma calcium levels at 1 to 2 h postadministration ($p < 0.001$), and a return of the calcium levels to baseline at 4 h postadministration (Figure 9). In contrast, all 6 rats administered with peroral REAL-sCT did

(24) Azria, M. *The calcitonins: physiology and pharmacology*; Karger: Basel; New York, 1989; pp vi, 152.

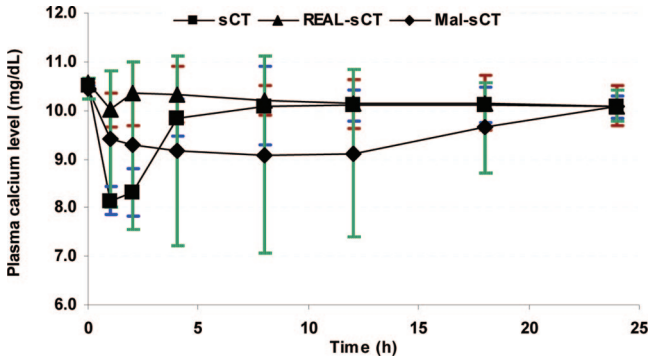

Figure 9. Plasma calcium level of rats administered with sCT, REAL-sCT and Mal-sCT by oral gavage. sCT and its conjugates dissolved in water at equivalent to 2.5 mg/mL of sCT, respectively, were dosed at 400 μL/rat (200 g). Data represent mean ± SD, $n = 6$.

not show lower plasma calcium levels from baseline values. These data contradicted an earlier report in which REAL-sCT administered as an emulsion was shown to have higher oral activity than sCT.[12] The present data indicate that REAL-sCT, without the aid of pharmaceutical excipients,[12] was not effective in lowering plasma calcium level when administered orally to rats. In the case of Mal-sCT, the in vivo results were mixed. While the majority of the rats (4 out of 6) did not exhibit a lowering in plasma calcium level following the administration of Mal-sCT, two rats in the group showed low calcium levels, about 6.5 mg/dL, from 2 to 12 h postadministration. Statistically, however, Mal-sCT, like REAL-sCT, did not show significant hypocalcemic activity after oral administration.

Pharmacokinetic Profile after Subcutaneous Injection. Figure 10 shows the plasma concentration of sCT, REAL-sCT and Mal-sCT following SC injection at a dose of 1.50, 1.81 and 1.90 mg/kg respectively in normal saline into Wistar female rats. The pharmacokinetic profile of sCT (Figure 10A) suggests a rapid elimination of the peptide from the circulatory system, the plasma sCT level decreasing from 150 nM at 10 min to an undetectable level (<1.3 nM) at 150 min. The rapid elimination of systemic sCT was not surprising given its susceptibility to hepatic metabolism. Rats injected subcutaneously with REAL-sCT showed gradually increasing REAL-sCT plasma concentration that reached a mean peak value of 419 nM at 150 min (Figure 10B). This concentration appeared to be sustained, for the mean plasma REAL-sCT concentration at 360 min was 473 nM. The rat plasma samples also recorded a concomitant rise in sCT concentration over the same time frame, suggesting that, even as REAL-sCT was absorbed from the injection site, sCT was being regenerated in the plasma. Mean plasma sCT concentration was 13.0 nM at 10 min postadministration, and ranged between 16 to 32 nM for up to 360 min. Since the plasma REAL-sCT concentration was around 10-fold higher than the sCT concentration, it was probable that the parent drug was regenerated from the lipidized peptide only after absorption into the systemic circulation. The greater persistence of REAL-sCT in the circulatory system was probably

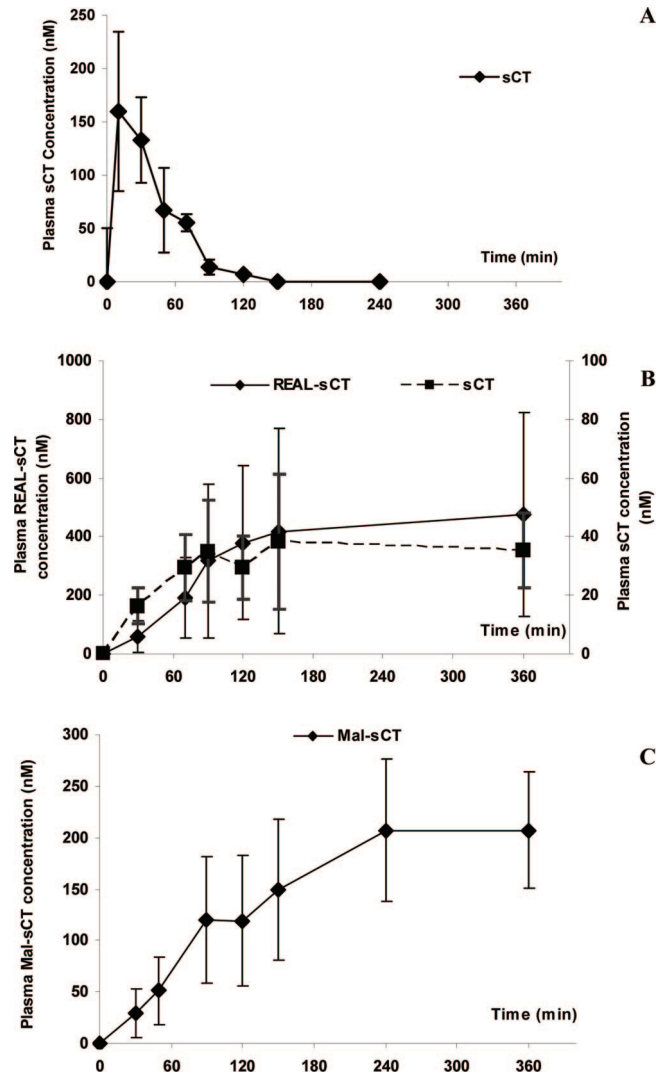

Figure 10. Plasma sCT, REAL-sCT and Mal-sCT concentration in Wistar female rats after a single SC injection of (A) sCT, (B) REAL-sCT and (C) Mal-sCT at the dose of 0.44 μmol/kg (equivalent to 1.50 mg/kg of sCT, 1.81 mg/kg of REAL-sCT and 1.90 mg/kg of Mal-sCT) in normal saline at the concentration of 0.44 μmol/mL. Data represents mean ± SD ($n = 3-4$).

due to its stronger resistance against hepatic metabolism compared to sCT. There was wide interindividual variation in plasma REAL-sCT concentration, which might be attributed to interindividual variation in hepatic enzyme activity.

In the Mal-sCT treatment group, there was a gradual buildup of plasma Mal-sCT over 240 min to reach a concentration of 207 nM, and this plasma concentration was subsequently maintained over the time frame of 240 to 360 min (Figure 10). The plasma Mal-sCT concentrations observed over the 90−360 min time points were comparable to the plasma sCT levels measured in the first 10−20 min for rats administered with sCT or REAL-sCT. In addition, the plasma Mal-sCT concentration−time profile paralleled that of the plasma REAL-sCT concentration−time profile measured through the 360 min postadministration. At all time

points measured, sCT was not detectable in the plasma samples of rats administered with Mal-sCT.

Discussion

Mal-sCT and REAL-sCT were successfully synthesized based on previously reported methods, their identities and purities being confirmed with ESI-MS and HPLC, respectively. As the two conjugates contained the same lipid groups, it was not surprising that they showed similar lipophilicities, as demonstrated by their comparable retention times under the same HPLC analytical conditions. The two sCT conjugates also showed similar secondary structures, which were robust and relatively independent of the solvent system compared to sCT. Unlike sCT, the lipidized sCT derivatives formed aggregates in water, a phenomenon that was likely driven by their lipophilic microenvironment.

Despite the similar backbone structures and lipophilicities, however, TEM micrographs and DLS measurements suggest that REAL-sCT and Mal-sCT showed different aggregation behaviors. REAL-sCT formed aggregates that were more than 10 times larger than Mal-CT, and, unlike Mal-sCT, REAL-sCT did not appear to dissociate into monomers when diluted from 1000 to 2.5 μM. The reason for the different aggregation behavior is not known, but it was apparent that the aggregation behavior of the lipidized sCTs could not be accounted for solely by lipophilicity.

Aggregation behavior is common for proteins and peptides, especially at high concentrations.[25–27] The aggregation of nonlipidized proteins commonly involves unfolding of native secondary and/or tertiary structure, and the increased formation of the β-sheet structure. Human calcitonin (hCT), the endogenous calcitonin present at approximately 0.3 mM in human, tend to spontaneously form aggregated fibrils in 20 min when dispersed in water.[28] On the other hand, this study has shown sCT at 1.0 mM to exist as monomers in water, a finding that is in agreement with a previous report, which showed sCT at 1.0 mM to be stable without evidence of aggregation for 7 months.[28] The difference in aggregated fibrillation behaviors between hCT and sCT was likely due to the very high p*I* value of sCT, at approximately 10.4.[29] At pH 5.0−7.0, sCT could form nonreversible aggregated fibrils at a concentration of 2 mM in the presence of EDTA, which facilitated a bridging aggregation of the acid groups and the amino groups of sCT.[29] The aggregation of hCT and sCT, either spontaneously or induced by EDTA, has been proposed to be both initiated and stabilized by the formation of the β-sheet structure at the C-terminal regions.[28,29] In the case of REAL-sCT and Mal-sCT, however, the morphology of the aggregates and the underlying mechanism for aggregation could be strikingly different, as the The REAL-sCT and Mal-sCT aggregates did not appear to form fibrils, and both lipidized sCT showed robust helical structures rather than the β-sheet structure.

Lipidization of peptides has not been unanimously translated to enhanced peptide stability against enzyme degradation. For example, the lipidization of SR-42128 (a pentapeptide rennin inhabitor) by dipalmitoyl glyceride modification at the C-terminal resulted in much increased intestinal and gastric stability,[4] but a similar lipidization of insulin decreased the peptide stability in intestinal fluid by 1.9-fold.[7] Similarly, while the REAL-lipidization of desmopressin with palmitic acid increased stability against liver enzymes, lipidization with hexanoic acid and decanoic acid decreased the peptide stability.[11] The underlying reasons for the variable outcomes are not well established. In our study, both REAL-sCT and Mal-sCT were more stable than sCT in the rodent liver and intestinal fluids. This is probably due to the propensity of the lipidized sCT to aggregate in aqueous media, which would restrict access by degradation enzymes. However, the degree of protection offered by the lipid conjugation, whether reversible or irreversible, was relatively modest. Due to the reversibility of REAL-sCT in liver juice, it was also difficult to compare the enzymatic stability of the two lipidized peptides.

In vivo, subcutaneously administered REAL-sCT and Mal-sCT at comparable doses exhibited comparable hypocalcemic intensities as sCT; however, REAL-sCT tended to induce a longer duration of hypocalcemic activity, for at least up to 24 h. The underlying mechanism of prolonged activity for REAL-sCT was elucidated by a pharmacokinetic study, using a novel LC−MS/MS method developed for the simultaneous detection of sCT and its conjugates in the same plasma sample. The LC−MS/MS method is advantageous over immunological methods, such as the radioimmunoassay (RIA) and enzyme-linked immunosorbent assay (ELISA), which can detect only intact, unmodified peptide drugs.[30] The LC−MS/MS method is also advantageous over a previously reported LC−ESI-MS method based on selected ion monitoring (SIM), as the current method offers higher specificity as it detects not only the parent ion but also the daughter ions.[31] A comparison of the pharmacokinetic data

(25) Chi, E. Y.; Krishnan, S.; Randolph, T. W.; Carpenter, J. F. Physical stability of proteins in aqueous solution: mechanism and driving forces in nonnative protein aggregation. *Pharm. Res.* **2003**, *20* (9), 1325–36.

(26) Shire, S. J.; Shahrokh, Z.; Liu, J. Challenges in the development of high protein concentration formulations. *J. Pharm. Sci.* **2004**, *93* (6), 1390–402.

(27) Frokjaer, S.; Otzen, D. E. Protein drug stability: a formulation challenge. *Nat. Rev. Drug Discovery* **2005**, *4* (4), 298–306.

(28) Arvinte, T.; Cudd, A.; Drake, A. F. The structure and mechanism of formation of human calcitonin fibrils. *J. Biol. Chem.* **1993**, *268* (9), 6415–22.

(29) Seyferth, S.; Lee, G. Structural studies of EDTA-induced fibrillation of salmon calcitonin. *Pharm. Res.* **2003**, *20* (1), 73–80.

(30) Buclin, T.; Cosma Rochat, M.; Burckhardt, P.; Azria, M.; Attinger, M. Bioavailability and biological efficacy of a new oral formulation of salmon calcitonin in healthy volunteers. *J Bone Miner. Res.* **2002**, *17* (8), 1478–85.

(31) Song, K. H.; An, H. M.; Kim, H. J.; Ahn, S. H.; Chung, S. J.; Shim, C. K. Simple liquid chromatography-electrospray ionization mass spectrometry method for the routine determination of salmon calcitonin in serum. *J. Chromatogr., B: Anal. Technol. Biomed. Life Sci.* **2002**, *775* (2), 247–55.

indicated a prolonged absorption phase (up to 240 min) for subcutaneously injected Mal-sCT and REAL-sCT, relative to the short T_{max} of 10 min obtained for similarly administered sCT. T_{max} for sCT was shorter than the values of 30−60 min reported by Sinko's laboratory for sCT injected subcutaneously at doses of 1 to 100 μg/rat.[21] The discrepancy could be caused by dose differences, the higher dose employed in our experiments resulting in greater concentration gradients that could have facilitated sCT absorption from the injection site. Absorption rates for REAL-sCT and Mal-sCT were slower by comparison, probably due to hydrophobic interaction of the lipidized peptides with the local adipose tissue or albumin in subcutis,[5] and/or a slower rate of elimination compared to sCT. Another nonreversible lipidized peptide reported to have a prolonged absorption phases is NN304 or ϵ-Lys^{B29}-myristoyl, des(B30) human insulin, which had comparable T_{max} of 4 to 6 h after subcutaneous injection at 0.15 to 0.60 U/kg in human volunteers.[32]

With the novel LC−MS/MS method, it was possible also to observe a buildup of plasma sCT after the subcutaneous injection of REAL-sCT at a sCT equivalent dose of 1.5 mg/kg. However, the significantly lower plasma sCT levels, compared to REAL-sCT concentrations, indicated that only a small portion of the systemic REAL-sCT was converted to sCT. Since plasma does not offer a reductive environment,[33] regeneration of sCT from REAL-sCT could be mediated by disulfide exchange reactions with the glutathione and thioredoxin enzymes in the liver,[34] possibly in the liver endothelial cells and Kupffer cells, as these cells are mainly responsible for the degradation of exogenous materials.[35,36] Formation of sCT was unlikely to occur in the general circulation as it required a reductive environment, which could be provided by the high level of glutathione (GSH) coupled with low levels of oxidized glutathione (GSSG) in the cytosol.[34] To date, the subcellular locations of the putative reduction sites and the mechanisms by which the endocytosed macromolecules were reduced remained poorly understood.[37] However, transportation of sCT and its analogues into the cytosol could take place via scavenger receptor mediated endocytosis/transcytosis.[36,38]

The active form of sCT has been predicted to assume the helical conformation,[39,40] and our Mal-sCT activity results support this assumption. It is not inconceivable that REAL-sCT itself might also possess hypocalcemic activity because it also has a stable helical conformation. In addition to that, due to the regeneration of sCT, REAL-sCT showed prolonged activity compared to Mal-sCT. Compared with sCT, Mal-sCT after subcutaneous injection generated higher plasma concentrations that persisted for a longer time, yet the duration of hypocalcemic activity shown by Mal-sCT was similar to that of sCT. On this basis, it might be concluded that Mal-sCT could have inferior potency compared to sCT.

Despite their inherent hypocalcemic activity and enhanced enzymatic stability, REAL-sCT and Mal-sCT did not provide statistically significant oral activity. Several reasons could account for this. Given that a typical GIT transit time is in the range of more than 1 h[41] and the concentration of enzymes in the GIT is much higher than that used in the in vitro experiments, it was likely that there was insufficient intact REAL-sCT and Mal-sCT remaining in the GIT for absorption into the systemic circulation following oral administration. Moreover, the lipid conjugates could form large aggregates in vivo, and these would have difficulty permeating the absorptive mucosa via the size-dependent passive diffusion pathway[42] unless the monomeric lipidized peptide was released. Although absorption via the transcytosis pathway, which was MW-independent as long as the aggregates had diameter of $\leq$100 nm,[43,44] was a possibility,

(32) Heinemann, L.; Sinha, K.; Weyer, C.; Loftager, M.; Hirschberger, S.; Heise, T. Time-action profile of the soluble, fatty acid acylated, long-acting insulin analogue NN304. *Diabetic Med.* **1999**, *16* (4), 332–8.

(33) Saito, G.; Swanson, J. A.; Lee, K. D. Drug delivery strategy utilizing conjugation via reversible disulfide linkages: role and site of cellular reducing activities. *Adv. Drug Delivery Rev.* **2003**, *55* (2), 199–215.

(34) Gilbert, H. F. Thiol/disulfide exchange equilibria and disulfide bond stability. *Methods Enzymol.* **1995**, *251*, 8–28.

(35) Smedsrod, B.; Pertoft, H.; Gustafson, S.; Laurent, T. C. Scavenger functions of the liver endothelial cell. *Biochem. J.* **1990**, *266* (2), 313–27.

(36) Jansen, R. W.; Molema, G.; Harms, G.; Kruijt, J. K.; van Berkel, T. J.; Hardonk, M. J.; Meijer, D. K. Formaldehyde treated albumin contains monomeric and polymeric forms that are differently cleared by endothelial and Kupffer cells of the liver: evidence for scavenger receptor heterogeneity. *Biochem. Biophys. Res. Commun.* **1991**, *180* (1), 23–32.

(37) Feener, E. P.; Shen, W. C.; Ryser, H. J. Cleavage of disulfide bonds in endocytosed macromolecules. A processing not associated with lysosomes or endosomes. *J. Biol. Chem.* **1990**, *265* (31), 18780–5.

(38) Van Berkel, T. J.; De Rijke, Y. B.; Kruijt, J. K. Different fate in vivo of oxidatively modified low density lipoprotein and acetylated low density lipoprotein in rats. Recognition by various scavenger receptors on Kupffer and endothelial liver cells. *J. Biol. Chem.* **1991**, *266* (4), 2282–9.

(39) Wang, Y.; Dou, H.; Cao, C.; Zhang, N.; Ma, J.; Mao, J.; Wu, H. Solution structure and biological activity of recombinant salmon calcitonin S-sulfonated analog. *Biochem. Biophys. Res. Commun.* **2003**, *306* (2), 582–9.

(40) Motta, A.; Pastore, A.; Goud, N. A.; Castiglione Morelli, M. A. Solution conformation of salmon calcitonin in sodium dodecyl sulfate micelles as determined by two-dimensional NMR and distance geometry calculations. *Biochemistry* **1991**, *30* (43), 10444–50.

(41) Christmann, V.; Rosenberg, J.; Seega, J.; Lehr, C. M. Simultaneous in vivo visualization and localization of solid oral dosage forms in the rat gastrointestinal tract by magnetic resonance imaging (MRI). *Pharm. Res.* **1997**, *14* (8), 1066–72.

(42) Goldberg, M.; Gomez-Orellana, I. Challenges for the oral delivery of macromolecules. *Nat. Rev. Drug Discovery* **2003**, *2* (4), 289–95.

(43) Sang Yoo, H.; Gwan Park, T. Biodegradable nanoparticles containing protein-fatty acid complexes for oral delivery of salmon calcitonin. *J. Pharm. Sci.* **2004**, *93* (2), 488–95.

this did not appear to occur to a significant extent. The poor correlation of data brings into question the validity of predicting in vivo oral activity based on in vitro stability results, as has been commonly practiced in the field.[4,45,46] In addition, a previous study[12] has found REAL-sCT to possess similar hypocalcemic activity as sCT when administered orally with Liposyn (an intravenous emulsion) as vehicle. This formulation of REAL-SCT was even shown to be more potent in inhibiting bone resorption than sCT after subcutaneous and oral administration. The discrepancy between the findings in the present study and that in the earlier study underpins the importance of formulation on the oral bioavailability of REAL-sCT. Further study is therefore necessary to establish the role of the lipid in the absorption profile of lipidized sCT.

(44) Desai, M. P.; Labhasetwar, V.; Walter, E.; Levy, R. J.; Amidon, G. L. The mechanism of uptake of biodegradable microparticles in Caco-2 cells is size dependent. *Pharm. Res.* **1997**, *14* (11), 1568–73.

(45) Yodoya, E.; Uemura, K.; Tenma, T.; Fujita, T.; Murakami, M.; Yamamoto, A.; Muranishi, S. Enhanced permeability of tetragastrin across the rat intestinal membrane and its reduced degradation by acylation with various fatty acids. *J. Pharmacol. Exp. Ther.* **1994**, *271* (3), 1509–13.

(46) Pardakhty, A.; Varshosaz, J.; Rouholamini, A. In vitro study of polyoxyethylene alkyl ether niosomes for delivery of insulin. *Int. J. Pharm.* **2007**, *328* (2), 130–41.

In summary, this study compared the biophysical properties of a reversible lipid conjugate of salmon calcitonin (REAL-sCT) and its nonreversible counterpart (Mal-sCT). Both of the conjugates showed stable helical conformations and a tendency to form aggregates in aqueous solutions. They were also more stable against degradation in rodent liver and intestinal fluids than sCT. REAL-sCT showed a more prolonged hypocalcemic activity than Mal-sCT after subcutaneous injection as aqueous solutions in the rat. Detectable levels of sCT was observed in plasma following the subcutaneous administration of REAL-sCT, but not Mal-sCT. Both lipidized sCT conjugates failed to show significant hypocalcemic activity following oral administration as aqueous solutions.

Acknowledgment. This research was supported by a National University of Singapore Academic Research Fund (R148-000-045-112). W.C. is grateful to the National University of Singapore for financial support of his graduate studies. The authors thank Dr. Seetharama D. S. Jois (Department of Basic Pharmaceutical Sciences, University of Louisiana at Monroe) and Dr. J. Sivaraman (Department of Biological Sciences, NUS) for their helpful discussion on the circular dichroism and DLS data, respectively.

MP8000167